Chapter 14
Cellular Automata for Simultaneous Analysis and Optimal Structural Topology Design

Zafer Gürdal and Ramzi Zakhama

14.1 Introduction

The Cellular Automata (CA) paradigm has been finding more and more applications in engineering and sciences in the past decade, but nevertheless its use for engineering design has not been widely popular. The proposed chapter is a special and unique implementation of the paradigm for combined analysis and design of continuum structures made of isotropic and fiber reinforced orthotropic materials. In particular, the use of a computational approach for topology design of the structural domain together with its local field and design variables is discussed.

Topology design of load carrying engineering structures has been one of the areas that have gaining popularity in the design engineering community. Current state of the art design tools enable engineers to define the boundaries of solid domains, providing them with useful tools for preliminary design. However, such boundaries are still rather course, even for two-dimensional domains let alone three-dimensional parts, due to computational efficiency of such tools. Of course the need and the drive for future development of these tools is to achieve a high level of resolution in part details, and be able to address not only structural load carrying functionality during design but also address other features, be it response to other non-mechanical and multidisciplinary loads (wind loads and thermal, magnetic and electric fields) or manufacturability.

The lack of computational efficiency mentioned above can be attributed to two restrictive features of most currently used design tools. The first is the inherently serial nature of both the analysis and the design algorithms. Most available topology optimization algorithms do not benefit from the computational efficiency that can be achieved from massively parallel implementations. This is primarily due to the difficulties associated with parallelizing the analysis routines that need to be executed after design changes. Developers of the optimization tools typically rely on off-the-shelf finite element analyses that either cannot be parallelized due to restricts

Z. Gürdal (✉)
Faculty of Aerospace Engineering, Delft University of Technology, Delft, The Netherlands
e-mail: z.gurdal@tudelft.nl

A.G. Hoekstra et al. (eds.), *Simulating Complex Systems by Cellular Automata*,
Understanding Complex Systems, DOI 10.1007/978-3-642-12203-3_14,
© Springer-Verlag Berlin Heidelberg 2010

access to their solvers, or simply do not scale well in terms of parallelization. Moreover, the number of design variables increases as the domain is discretized into smaller and smaller parts to achieve higher design resolution. The immediate outcome of this restriction makes the design optimization extremely computationally demanding due to what is commonly referred to as the *curse of dimensionality*. The second limitations is the perceived notion that a design process is simply performing repetitive analyses and monitoring the performance of the design while maintaining constraint satisfaction during the process. Of course engineers currently have very fast analysis tools that can evaluate the performance of a design to a large degree of precision. Nevertheless, even though they are fast, it is probably not justified to perform an engineering analysis of a part to such high precisions if one is going to toss away the result as soon as the design is modified to improve it. It can be argued that an efficient engineering design requires its own computational paradigm that enables computation of topologies without the use of time consuming high precision analyses.

The growing interest in solving complex problems using CA has recently found its implementation in complex structural design problems. The paradigm appears to address most of the limitations described above based on features well described in the earlier chapters of this book. Kita and Toyoda [1] were among the first to use the cellular automata paradigm for solving topology optimization problems. They constructed CA design rules to obtain two-dimensional topologies based on an Evolutionary Structural Optimization (ESO) approach [2, 3]. In their approach the analysis of the structure however is performed using the Finite Element method.

Another pioneering work is attributed to Gürdal and Tatting [4] who used the CA paradigm to perform an integrated analysis and design. They solved the topology and sizing design of trusses that exhibit linear and geometrically nonlinear responses. The analysis rules are derived from local neighborhood equilibrium, while a simple design rule that is based on fully stressed design (a Stress Ratio (SR) method) [5] is used to size the truss members, in which the cross sectional areas of the members that connect the neighboring cells were the design variables.

The concept was later extended to preliminary implementation of the design of two-dimensional continuum structures by Tatting and Gürdal [6]. At the cell level the two-dimensional continuum is modeled by a truss layout that is equivalent to the continuum cell according to an energy criterion. The relationship between the thickness of the continuum structure and the cross sectional areas of the truss members is established by equating the strain energy of the continuum cell and that of the truss cell for given nodal displacements. The local analysis rules are again derived from the equilibrium condition of the cell, and a fully stressed material condition is selected to construct the local design rule. Numerical examples are carried out and results compared to an iterative Finite Element Analysis based design scheme that used GENESIS software to demonstrate the efficiency of the combined CA analysis and design.

Encouraged by the success of applying the CA paradigm to structural design, Abdalla and Gürdal [7] extended CA to the design of an Euler-Bernoulli column for minimum weight under buckling constraint, which is an eigenvalue problem. Global nature of eigenvalue problems, and its reduction to local analysis and design rules were the principal contribution of the work. The analysis rule is derived by minimization of the total potential energy in a cell neighborhood and the design rule is formulated as a local mini-optimization problem involving force resultants. The proposed CA algorithm is shown to converge correctly to an analytical optima for a number of classical test cases.

A more formed treatment of the problem of topology optimization of an elastic two-dimensional plate appeared first in Abdalla and Gürdal [8]. In their work, CA design rule is formulated for the first time using rigorous optimality criteria based on SIMP material [9–13] approach. The CA analysis rule was derived from the principle of minimal total potential energy. An extension of this work was made by Setoodeh et al. [14] to combine fiber angle and topology design of an anisotropic fiber reinforced laminae. Fibre angles and density measures at each cell of a domain are updated based on the optimality criteria for the minimum compliance. Topology optimization of 2-D elastic continuum structures subject to in plane loads and exhibiting geometric nonlinearities was performed by Zakhama et al. [15].

The cellular automata paradigm is also well known to be an inherently massively parallel algorithm. Slotta et al. [16] have implemented Gürdal and Tatting's [4] work using standard programming languages and parallelization libraries. The domain is decomposed into different groups of cells. Each group is assigned to a processor and the same local rules are applied for all the processors. Results demonstrate that the CA method is perfectly suited for parallel computation. Setoodeh et al. [17] proposed solving topology optimization for a continuum structure using a pipeline parallel implementation of cellular automata on distributed memory architecture. Numerical results show that the pipeline implementation converges successfully and generates optimal designs.

For the above mentioned structural analysis and design studies it has been observed that the CA convergence rate deteriorates considerably as the cell density is refined. This is due to the slow propagation of cell level field variables across the structural domain governed by elliptic partial differential equations. Additionally when a CA algorithm is implemented on a serial machine it looses its most attractive feature- parallelism [16, 17]. A methodology based on the Multigrid scheme can be used to accelerate the CA convergence process on serial machines. It has been demonstrated that the CA method takes advantage of the acceleration effect of multigrid schemes [18, 19]. The main idea in the multigrid concept is to use different discretization levels of cell grids, where the iterations of a classical iterative method on the finer grid are coupled with the iterations for the correction of the solution on the coarser grids. This concept is illustrated in depth by Wesseling [20].

Tovar et al. [21] have proposed another alternative to accelerate the CA convergence. The authors proposed a scheme based on Finite Element method to accelerate the analysis process followed by CA design rule. This type of strategy is often called

Hybrid Cellular Automata (HCA). In their paper, the CA local design rules are based on control theory, which minimizes the error between a local Strain Energy Density (SED) and the averaged SED value. More recently, Tovar et al. [22] have derived the CA local design rules based on optimality criteria interpreted as Kuhn-Tucker conditions of a multi-objective problem in addition to the control theory defined earlier in [21].

In the following basic elements of the definitions that are specific to topology design optimization of structural domains is described. In particular, sections on local rules that will ensure local equilibrium for analysis purposes and optimality for design purposes are described. Numerical implementation for the cellular automata paradigm for different type of structures are presented. Examples describing engineering applications are provided starting with two- and three-dimensional isotropic domains with local density design variables, followed by anisotropic medium in which local design variables in the form of fiber orientation angles is used in addition to the density variables.

14.2 Modeling for Structural Analysis and Design

For structural analysis and design local cell state will include physical and geometric properties of a solid domain. Principal response quantities (i.e., unknown field variables) of the analysis effort of a solid domain is typically the displacements. Local geometry of the cell are typically cross-sectional areas, cell densities, fiber-angle orientation, etc., which represent the design variables associated with the cell. In addition, local tractions applied to the cell and material properties of the solid may be needed for computations, and constitute part of the cell state, even if they may not be changing during the calculations.

A structural domain can be 1-,2- or 3-Dimensional, In the present chapter the trivial 1-D structures such as beams and columns [7, 18] are ignored, putting the emphasis on 2- and 3-D domains. Such domains can be of discrete nature, such as a truss type structure [4, 16, 23, 24], or a continuum type [6, 8, 14, 15, 17, 19, 25], such as plate and shell type structures. In the following basic description of the CA representation of these different kinds of structural domains are provided.

14.2.1 Truss Domain

Following the basic elements of the CA methodology described in Chap. 1, the cell representation of a simple 2-D discrete structural domain is a ground truss structure shown in Fig. 14.1a. In this representation, each cell is made up of eight truss members extending from the cell center at every 45° orientation. The Moore neighborhood with radius $r = 1$ is selected as shown in Fig. 14.1b. This neighborhood is composed of the eight adjacent cells which are marked by NW, N, NE, W, E, SW, S, and SE (see Fig. 14.1b) following the traditional compass representation

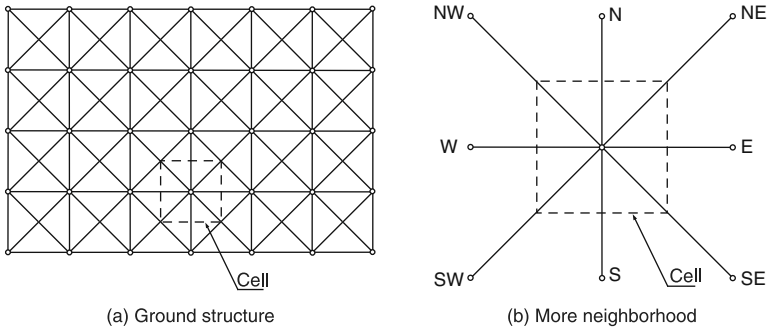

Fig. 14.1 CA ground structure and Moore neighborhood for trusses

of directions. For 2-D structural analysis the primary field variables are the nodal displacement components at truss junctions. The cell state also depends on the geometric and material properties of the truss members as well as the applied external loads at the truss nodes. Hence the cell state in the present application consists of two displacement components in mutually orthogonal directions, cross sectional areas of eight bars attached to the cell, and external loads in the two primary direction of the domain. In the present example the material type of the members is assumed to be fixed and kept outside the state of the cell that will change iteratively. Following the notation introduced in Chap. 1, the definition of the cell state at a given time iteration can be defined as

$$\Sigma(i) = \left\{(u_i, v_i), \left(f_i^x, f_i^y\right), \left(A_i^{\mathrm{NW}}, A_i^{\mathrm{N}}, A_i^{\mathrm{NE}}, A_i^{\mathrm{W}}, A_i^{\mathrm{E}}, A_i^{\mathrm{SW}}, A_i^{\mathrm{S}}, A_i^{\mathrm{SE}}\right)\right\}, \tag{14.1}$$

where u_i and v_i are the horizontal and vertical displacements, respectively. The reaction forces are denoted by f_i^x and f_i^y in the x and y directions respectively, and the member areas are represented by $A_i^{\mathrm{NW}}, A_i^{\mathrm{N}}, \ldots, A_i^{\mathrm{SE}}$.

The boundary condition mentioned in Chap. 1 is chosen as fixed for this example. To accomplish that, for cells at the boundary, cross sectional areas of the members which lie outside the structural domain are set to zero, which removes those truss members and provides a finite boundary for the truss ground structure. For the cell locations where the structure is physically restrained to prevent rigid body motion or restrained because of functional requirements, the appropriate displacement components are set to be zero and unchanging.

14.2.2 Isotropic Continuum Domain

In this section, the CA discretization of two and three dimensional structural domains is considered. The elastic continuum domain is discretized by a lattice of regular cells which are equally spaced in the x and y directions (see Fig. 14.2a), or

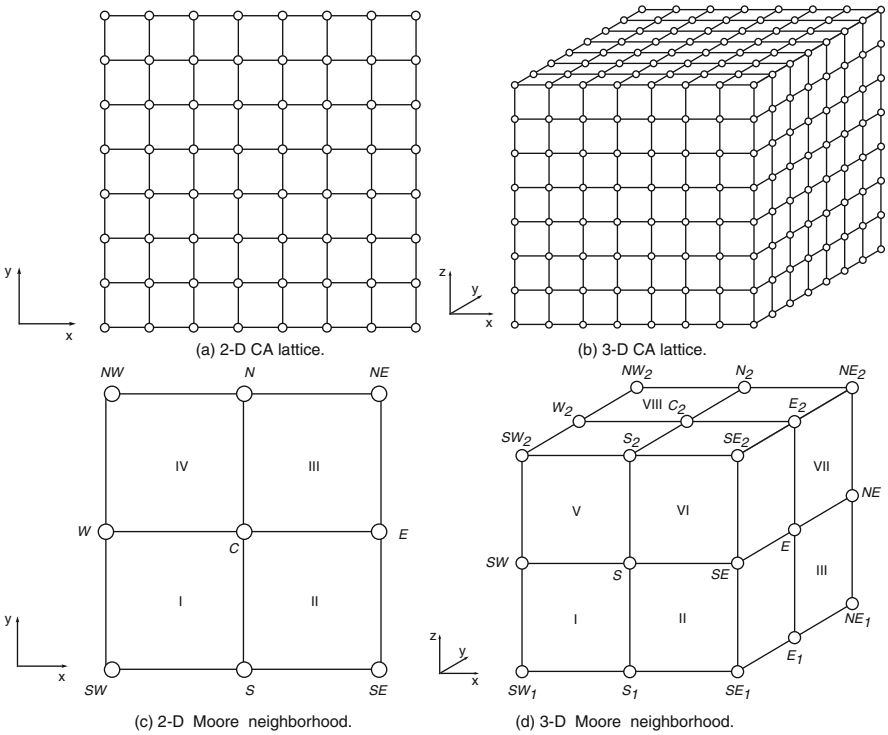

Fig. 14.2 CA lattices and Moore neighborhood for continuum structures

x, y and z for a three-dimensional structural domain (see Fig. 14.2b). Traditional Moore neighborhood is used to define the connectivity of the lattice as shown in Figs. 14.2c and 14.2d. In this case, the neighborhood includes the entire are, numbered by roman numerals, between the cell points again represented by the compass directions.

Each center cell C_i communicates with its neighbors by a local rule and its state is denoted as $\Sigma(i)^{(t)}$ where t is the iteration number. For isotropic continuum topology structures in two and three dimensions, the state of the ith cell is defined by

$$\Sigma(i) = \left\{ \left(u_i^{(1\ldots m)} \right), \left(f_i^{(1\ldots m)} \right), \rho_i \right\}, \tag{14.2}$$

where m corresponds to the dimensionality of the domain, with $m = 2$ or 3 for two or three dimensional domains, respectively. The components $\left(u_i^{(1\ldots m)} \right)$ are the cell displacements in the directions $(1\ldots m)$, and $\left(f_i^{(1\ldots m)} \right)$ the external forces acting on the ith cell in the respective $(1\ldots m)$ directions. Each cell of the discretized domain has its own density measure ρ_i at the node point independently of the densities of the elements numbered by roman numerals that define the neighborhood.

14.2.3 Composite Lamina Continuum Domain

A special case of a 2-D continuum is orthotropic fiber reinforced composite laminates in which the fibers provide stiffness and strength in preferred directions. Hence, determining the fiber orientation angle is an important part of the design; activity that is commonly referred to as *tailoring*. For combined topology and fiber-angle design, the basic CA elements of the isotropic continuum domain remain almost the same, however, the state of the ith cell is modified as follows:

$$\Sigma(i) = \left\{ \left(u_i^{(1...m)} \right), \left(f_i^{(1...m)} \right), (\rho_i, \theta_i), \overline{\mathbf{Q}}_i \right\}, \tag{14.3}$$

where θ_i is the fiber angle of the ith cell and $\overline{\mathbf{Q}}_i$ is the reduced transformed stiffness in which, due to symmetry, only the upper half diagonal of the matrix is stored.

14.3 Analysis Update Rule

14.3.1 Truss Structures

Local analysis rule is derived from the equilibrium condition of a cell with its neighbors. Within a cell, each truss member of the neighborhood structure ($k = 1, ..., 8$) has a Young modulus E, a length L_i^k before deformation, and a cross-sectional area A_i^k. The total potential energy associated the cell is the sum of the strain energy in each of the eight truss member of the neighborhood structure, as well as the potential energy of the external forces applied to the cell:

$$\Pi_i = \sum_{k=1}^{8} \frac{E\ A_i^k\ L_i^k\ (\varepsilon_i^k)^2}{2} - f_i^x\ u_i - f_i^y\ v_i, \tag{14.4}$$

where ε_i^k is the truss member strain which depends on the relative displacements of the neighboring cells. The strain is evaluated using the Green's strain definition for a truss members:

$$\varepsilon_i^k = \frac{(u_i - u_i^k)cos\theta^k - (v_i - v_i^k)sin\theta^k}{L_i^k}, \tag{14.5}$$

where (u_i^k, v_i^k) are the neighboring displacements, and θ^k is the orientation angle of the kth truss element member from the cell center.

Thus, the equilibrium equations are obtained by minimizing the total potential energy with respect to the cell displacements u_i and v_i:

$$\frac{\partial \Pi_i}{\partial u_i} = 0, \qquad \frac{\partial \Pi_i}{\partial v_i} = 0. \tag{14.6}$$

14.3.2 Isotropic Continuum Structures

The equilibrium of the neighborhood structure (see Figs. 14.2c,d) is again used to formulate the local analysis update rule. The total potential energy associated with a cell is the sum of the strain energy in each element of the neighborhood structure and the potential energy due to the external forces applied directly to the cell. Note that in this discretization scheme there will only be a few cells in the domain at which external forces are applied. Most cell equilibrium will only involve interaction of the local cells through the solid domain between them, which following the terminology of finite element analysis are referred to as the elements in this chapter:

$$\Pi_i = \sum_{k=1}^{N_{\text{element}}} U_i^k - \mathbf{f}_i \cdot \mathbf{u}_i, \tag{14.7}$$

where N_{element} is the number of elements surrounding a cell represented by the roman numerals in the figure, U_i^k is the strain energy for the kth element, $\mathbf{f}_i$ is the applied force vector and $\mathbf{u}_i$ is the displacement vector for all the cell's neighborhood including the cell itself.

The strain energy of an element is expressed in terms of the strain energy of the base material as follows:

$$U^k = \bar{\rho}^p \tilde{U}, \tag{14.8}$$

where

$$\tilde{U} = \frac{1}{2} \int_{\text{element}} \Gamma \cdot \overline{\mathbf{Q}} \cdot \Gamma \; dxdydz, \tag{14.9}$$

is the strain energy of the base material, Γ is the small-strain tensor, and $\overline{\mathbf{Q}}$ is the reduced in-plane stiffness matrix. The symbol p in the equation is called penalization parameter and is used for design purposes, its role will be explained later in the design rules.

The elements densities $\bar{\rho}$ are obtained by an average density interpolation [8] given by

$$\frac{1}{\bar{\rho}^p} = \frac{1}{N_{\text{cell}}} \sum_{i=1}^{N_{\text{cell}}} \frac{1}{\rho_i^p}, \tag{14.10}$$

where ρ_i's are the density measures of the cells surrounding the element, and N_{cell} is the number of cells defining the element. For the two-dimensional neighborhood structure $N_{\text{cell}} = 4$ and for the three-dimensional neighborhood structure $N_{\text{cell}} = 8$.

The density interpolation scheme in the previous equation is chosen such that any node with a density measure below a threshold value would *turn off* all four

elements in which the node participates. Using this scheme checkerboard patterns are suppressed automatically during the optimization process.

Equilibrium equations are obtained by minimizing the total potential energy with respect to the cell displacements:

$$\min_{\mathbf{u}_C} \Pi_i . \tag{14.11}$$

The resulting equilibrium equations for each cell are written in a residual form:

$$\mathbf{R}_C(\mathbf{u}_C, \mathbf{u}_N) = \begin{Bmatrix} \mathbf{G}_C(\mathbf{u}_C, \mathbf{u}_N) \\ \mathbf{G}_N(\mathbf{u}_C, \mathbf{u}_N) \end{Bmatrix} + \begin{Bmatrix} \mathbf{f}_C \\ \mathbf{f}_N \end{Bmatrix} = 0, \tag{14.12}$$

where $\mathbf{u}_C$ and $\mathbf{u}_N$ are the displacement vectors of the cell and the neighborhood, respectively, $\mathbf{G}_C$ and $\mathbf{G}_N$ are the vectors of the internal forces, $\mathbf{f}_C$ and $\mathbf{f}_N$ are the vector of the applied forces relative to the cell and the vector of the internal forces relative to the neighborhood, respectively.

Differentiating the vector $\mathbf{R}_C$ with respect to the components of $\mathbf{u}_C$, the linear stiffness matrix can be written as

$$\mathbf{K} = -\frac{\partial \mathbf{R}_C}{\partial \mathbf{u}_C}(\mathbf{u}_C, \mathbf{u}_N). \tag{14.13}$$

The stiffness matrix $\mathbf{K}$ can also be expressed as the Hessian of the total potential energy:

$$\mathbf{K}_{pq} = \frac{\partial^2 \Pi_i}{\partial u_p \, \partial u_q}. \tag{14.14}$$

Thus, the cell displacements are updated as follows:

$$\mathbf{u}_C^{t+1} = \mathbf{u}_C^t + \triangle \mathbf{u}_C, \tag{14.15}$$

$$\triangle \mathbf{u}_C = (\mathbf{K}_C)^{-1} \cdot \left(\mathbf{G}_C(\mathbf{u}_N^{t+1}) + \mathbf{f}_C \right), \tag{14.16}$$

where $\mathbf{K}_C$ is a (2×2) or (3×3) cell stiffness matrix for two or three dimensional cases, respectively.

14.3.3 Composite Lamina Continuum Structures

When considering fiber-angle in the topology optimization problem the same formulation described above is used, with the only exception that now the fiber orientation is allowed to change from cell to cell. This changes the computation of the reduced in-plane stiffness, which is obtained as follows:

$$\overline{\mathbf{Q}} = \frac{1}{N_{\text{cell}}} \sum_{i=1}^{N_{\text{cell}}} \overline{\mathbf{Q}}_i, \tag{14.17}$$

where $\overline{\mathbf{Q}}_i$ is the in-plane transformed reduced stiffness of the four nodes of the element.

Thus, the analysis update rule is performed as described earlier using (14.15).

14.4 Design Update Rule

Structural analysis is based on a fairly well established principles and mathematical formulation that results in well know partial differential equations. Hence, the analysis rules described above are derived using the same principles. The design world on the other hand is much less restrictive, and there are variety of possibilities that one can implement design changes during an iterative scheme. The possibilities range from purely heuristic changes to, simple pattern matching, or to formal mathematical formulation. In the following, implementation of the design rules for the the three cases that we are discussing are presented.

14.4.1 Truss Structures

The design update rule in this case is derived from resizing the truss element members of the neighborhood structure based on full utilization of load carrying capability of the material. The cross sectional update formula is commonly referred to as the *fully stressed design* or *stress ratio* approach [5]. This scheme consists on computing a new cross sectional area $(A_i^k)^{(t+1)}$ which is based on the previous cross sectional area $(A_i^k)^{(t)}$ and the allowable stress σ_{all} chosen by the user as the maximum stress that the material can carry:

$$(A_i^k)^{(t+1)} = (A_i^k)^{(t)} \frac{E\,|\varepsilon_i^k|}{\sigma_{\text{all}}}. \tag{14.18}$$

14.4.2 Continuum Structures

The structural topology design problem is posed according to the minimal compliance formulation. Its aim is to minimize the elastic strain energy of the structure, or equivalently maximize its total potential energy Π at equilibrium, subject to a limitation on the material volume. Thus, the design problem is written as

$$\min_{\rho} W_c(\rho, \mathbf{u}^*) \quad \text{or} \quad \max_{\rho} \Pi(\rho, \mathbf{u}^*), \tag{14.19}$$

under the constraints:

$$\mathbf{g}(\rho) \leq 0, \tag{14.20}$$

and the volume constraint:

$$\int_{\Omega} \rho \, d\Omega \leq \eta \cdot V_{\Omega}, \tag{14.21}$$

where ρ is the local density distribution of material which is chosen as the design variable, Ω is the prescribed design domain, $\mathbf{u}^*$ is the displacement vector at equilibrium, and $\mathbf{g}$ is a vector of local constraints which set bounds on the density distribution. The volume V of the structure is limited to an available fraction η of the total volume of the design material domain V_{Ω}. From the optimality conditions of the system level design problem (14.19), (14.20), and (14.21), local optimality conditions are derived which are associated with the cell level optimization problem. According to the specialization of the SIMP method, the local stiffness of the structure is expressed as a function of a fictitious local density distribution ρ. The local optimization problem takes on the form [8, 14]:

$$\min_{\rho} \frac{\Phi^*}{\rho^p} + \mu \, \rho, \tag{14.22}$$

$$\varepsilon \leq \rho \leq 1, \tag{14.23}$$

where

- $\varepsilon > 0$ is a very small number, set as a lower bound on ρ to avoid numerical instability that may result from structural discontinuities when zero density is allowed,
- $p \geq 1$ is a penalization parameter that is introduced in order to lead the design to a black or white topology, by assigning sufficiently high values to p, typically $p = 3$,
- $\Phi^* = \rho^p \, \hat{\Phi}$, is an approximately invariant local quantity, and $\hat{\Phi}$ is the complementary energy density,
- μ is the Lagrange multiplier associated with the global volume constraint (14.21). It is the only global quantity that is involved in this local problem. It serves in updating the material densities in the domain. It is updated at the global level by satisfying the total volume constraint [8, 14].

The update of each cell density of the continuum structure is obtained from the solution of this one-dimensional convex problem. The analytically solution [8, 14] of this local optimization problem is as follows:

$$\begin{cases} \hat{\rho} & \text{for} \quad \varepsilon < \hat{\rho} < 1 \\ \varepsilon & \text{for} \quad \hat{\rho} \leq \varepsilon, \\ 1 & \text{for} \quad \hat{\rho} \geq 1 \end{cases} \tag{14.24}$$

where

$$\hat{\rho} = \left(\frac{\Phi^*}{\bar{\mu}}\right)^{\frac{1}{1+p}}, \qquad \bar{\mu} = \frac{\mu}{p}. \tag{14.25}$$

The energy density Φ^* for each cell of the domain can be written as an average among the N_{element} elements of the Moore neighborhood structure:

$$\Phi^* = \frac{1}{n\,v} \sum_{i=1}^{N_{\text{element}}} \bar{\rho}_i^{2\,p}\,\tilde{U}_i, \tag{14.26}$$

where n is the number of non-shadow elements with nonzero density, v is the volume of a cell, which is $v = h^2$ or h^3 for two or three dimensional cases, respectively, and h is the distance between two immediate neighbor cells.

14.4.3 Composite Lamina Continuum Structures

By considering θ and ρ to be the design variables, we can convert the problem of combined topology and fibre-angle design to a local optimization problem through the general formulation (14.19), (14.20), and (14.21) as

$$\min_{\rho,\theta} \frac{\Phi(\theta)}{\rho^p} + \mu\,\rho, \tag{14.27}$$

$$\varepsilon \le \rho \le 1. \tag{14.28}$$

The value of $\Phi(\theta)$ is evaluated based on the current value of the cell density ρ and the strain vector Γ, and then used to update the local density through the solution of (14.27) and (14.28). Due to its special mathematical form, this local optimization problem can be easily split into two subproblems:
one for fibre-angle design,

$$\Phi^* = \min_{\theta} \Phi(\theta), \tag{14.29}$$

$$\Phi^* = \frac{1}{n\,v} \sum_{i=1}^{N_{\text{element}}} \bar{\rho}_i^{2\,p}\,\tilde{U}_i(\theta), \tag{14.30}$$

and the second one for topology,

$$\min_{\rho} \frac{\Phi^*}{\rho^p} + \mu\,\rho, \tag{14.31}$$

$$\varepsilon \le \rho \le 1. \tag{14.32}$$

It is well known that the optimal fiber-angle orientation for "shear weak" materials coincides with the principal stress direction [26, 27]. For "shear strong" materials there exists a closed form solution for which, depending on the principal strain ratio and material properties, the orientation might again coincide with principal stress direction or be different from the principal stress direction [26, 27].

In addition to the mathematical formulation of the fiber orientation angle update, it is also possible to use schemes that are less formal. For example, it is known that more than often incorporation of manufacturing requirements into mathematical formulations is not possible or will result in computationally expensive schemes that will be unaffordable. One such consideration is the continuity of the fiber orientation angle from one cell to another. In real life, fibers are continuous strands and abrupt change in orientation angle from one cell to another is not feasible. To account for such a requirement Setoodeh et al. [25] implemented a pattern matching technique, which re-updated the fiber orientation computed using the mathematical expressions with orientation angle patterns of the neighboring cells forming uniform orientation angle in the neighborhoods, with only well defined boundaries in the domain with different fiber orientation angles.

14.5 Cellular Automata Implementation Schemes

The update of the cells for trusses and continuum structures can be done simultaneously, which corresponds to the Jacobi scheme, as follows:

$$\Sigma(i)^{(t+1)} = \phi\left(\Sigma(i)^{(t)}, \Sigma(NM)^{(t)}\right), \tag{14.33}$$

or sequentially, which corresponds to Gauss-Seidel scheme:

$$\Sigma(i)^{(t+1)} = \phi\left(\Sigma(i)^{(t)}, \Sigma(M)^{(t+1)}, \Sigma(NM)^{(t)}\right), \tag{14.34}$$

where M is the set of neighboring cells whose states have been modified in the current iteration and NM is the set of remaining cells, which have not yet been modified.

The Gauss-Seidel method is used for the analysis update. For the design update, the Jacobi method is found to be the appropriate one to use to preserve the symmetry of the solution [8].

14.5.1 Truss Structures

The ground truss structure algorithm is based on the repeats of the analysis and design update rules for each cell of a domain. The algorithm starts from updating the displacement for a given structure until the norm of the force imbalance (residual) reaches a pre-specified tolerance ε_r. Then, the cross sectional areas are

updated using the design update rule. The algorithm has deemed to converge when the structural design no longer changes.

14.5.2 Continuum Structures

For the topology of continuum structures, the analysis and design iterations are nested. A flowchart of the CA design algorithm is presented in Fig. 14.3. Starting from a structure with zero displacements and from densities set to volume fraction η, analysis updates are performed repeatedly until the norm of the force imbalance (residual) reaches a pre-specified tolerance ε_r. Next, the design is updated over the whole domain, then the volume constraint is checked. If the volume constraint is not satisfied, the Lagrange multipliers are updated and so is the design. The process continues until the relative difference between five successive compliance values is less than a pre-specified tolerance ε_c and the variation in cell densities is less than a tolerance ε_d.

From a computational perspective, the attractive feature of CA is its inherent parallelism. This feature appears to be particulary effective with regard to the analysis update. When it is not fully exploited, CA algorithms can be quite slow to converge. This is because communication between cells is limited only to immediate neighbors. The information from the cells where the loads are applied has to travel by neighbor-to-neighbor interaction throughout the domain. As the lattice is refined, the number of lattice updates needed to reach equilibrium significantly increases manifesting the deterioration in the rate of convergence alluded to above. Thus,

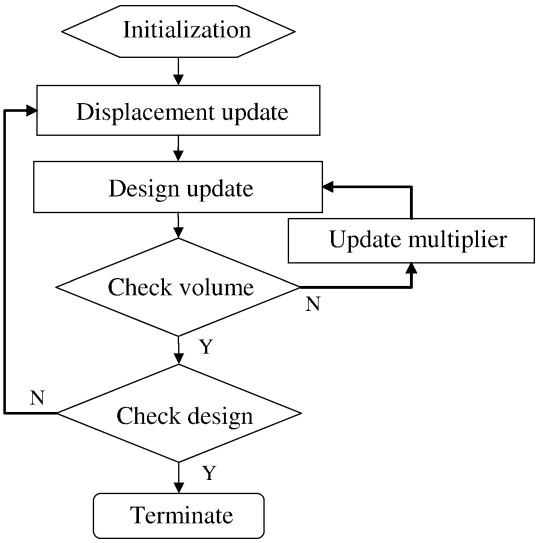

Fig. 14.3 CA continuum design algorithm

when CA is implemented on a serial machine it loses its most attractive feature as far as the analysis update is concerned. The design features of CA, though, remain effective.

An alternative methodology based on multigrid scheme [18–20] is used to accelerate the CA design algorithm on a serial machine. The multigrid acceleration scheme uses different discretization levels of grids. The CA iterations on the finest grid are coupled with the iterations of the correction solution on the coarse grids. The multigrid accelerated CA algorithm is demonstrated to be a powerful tool for solving topology optimization problems compared to other algorithms based on traditional finite element analysis [19]. The computational cost using this scheme is numerically found to be proportional to the number of cells.

14.6 Numerical Examples

In this section, some examples of topology optimization of continuum structures are considered to illustrate the robustness of the CA based combined analysis and design algorithm. As mentioned earlier the CA-based analysis is computationally expensive compared to an analysis using modern tools on a serial machine. Therefore, it is essential to implement CA in a parallel environment to exploit the true merits of a CA-based structural analysis and design. However, massively parallel computing machines that are most suited to this kind of computations are not as easily accessible as serial ones. To accelerate the convergence of CA iterations, two schemes are used in the present chapter. The first scheme is based on multigrid accelerated CA [19]. The second scheme is based on HCA, which uses a global finite element analysis instead of iterative updates of cell displacements followed by local update rules used for the design.

14.6.1 Example 1: 2-D Plate Topology Design

To demonstrate the performance and efficiency of the multigrid accelerated CA algorithm in solving the topology optimization problem, its results are compared with an existing method that is based on iterative finite element analysis solutions. Since the same CA design update rule is used in all tested algorithms, the comparison concerns design algorithms based on different analysis processes, namely the multigrid scheme and the commercial NASTRAN finite element code. The example studied is a symmetric cantilever (see Fig. 14.4) plate which is 1,000 mm long, 250 mm high, and 1 mm thick. The penalization parameter p is set to 3, the volume fraction is set to 0.5, the Poisson ratio is 0.4 and the Young modulus E is 1,000 $\mathrm{N/mm^2}$. The tip load considered is $P = 100$ N acting at the center point of the free end of the cantilever.

Different discretization levels are used for the comparison; the results are generated for 11 grid levels, starting from the coarsest grid level of 9×3 cells, up to

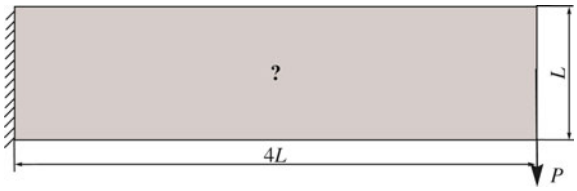

Fig. 14.4 Geometry and loading

the finest grid level of 4,097 × 1,025 cells. Convergence time for the HCA solution using the commercial NASTRAN code and for the multigrid accelerated CA algorithm are illustrated in Fig. 14.5. The vertical and horizontal axes represent the convergence time and the number of cells, respectively, on a log-log scale. First, it is observed that the commercial NASTRAN code showed a higher convergence time than the other algorithm. Moreover, the commercial NASTRAN code suffers lack of memory while running the grid level of 2,049 × 513 cells. On the contrary, the cellular automata paradigm can handle large problems because of its local nature which makes the storage of the global stiffness matrix unnecessary. The run time to convergence relative to the multigrid algorithm appears to be nearly proportional to the number of cells, which reveals a computational effort in the order of $O(N)$. As for the optimal topologies, it can be seen from Table 14.1 that those obtained by the multigrid algorithm and by the use of NASTRAN for analysis are practically the same with a slightly (0.005%–0.03%) but persistently lower compliance in the multigrid results.

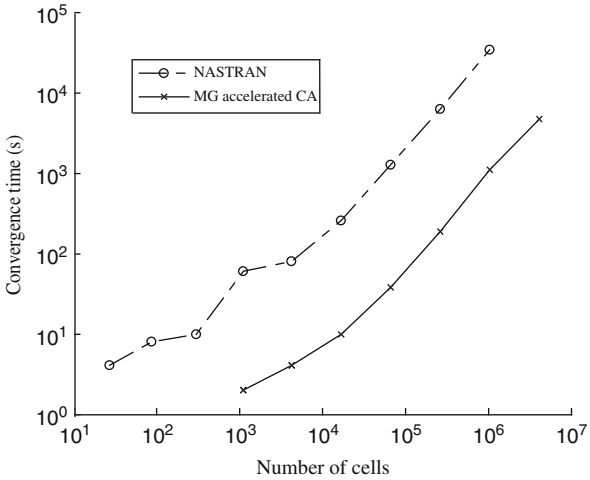

Fig. 14.5 Convergence time using NASTRAN and Multigrid accelerated CA

Table 14.1 Optimal topologies and compliances

Cell number	Optimal topology using NASTRAN	Optimal topology using Multigrid
129×33	4,273.6	4,258.7
257×65	4,064.1	4,062.7
513×129	3,985.7	3,984.2
1,025×257	3,983	3,980.9
2,049×513	3,994	3,992
4,097×1,025	Lack of memory	3,998.4

14.6.2 Example 2: 2- and 3-D Compression Bridge

In this example, the objective is to find an optimal topology for a bridge which crosses a river and supports a uniformly distributed traffic loading. The design domain, the loading and the boundary conditions of the bridge problem are represented in Fig. 14.6. Requirements of waterway traffic underneath and road traffic on the bridge translate into the definition of imposed zones: empty (void) zones for the waterway and vehicle traffic through the bridge, and a dense (black) one for the deck and supports, as represented in Fig. 14.6. The design domain is discretized with 257 × 65 cells for the two-dimensional case and with 257 × 65 × 33 for the three-dimensional case including the empty zone. The penalization parameter p is set to 3, the volume fraction is set to 0.1 and the Poisson ratio to 0.3.

The final topology for the two-dimensional case performed by the multigrid design algorithm is represented in Fig. 14.7. It corresponds to a compression arch which holds a three span deck. The first and the third spans are cantilevers which

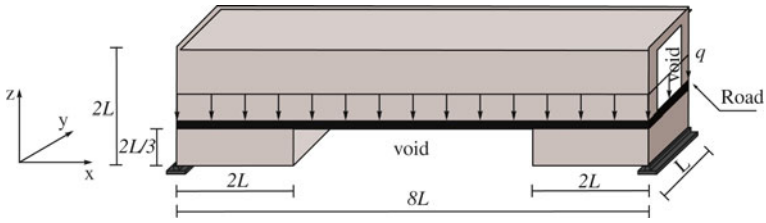

Fig. 14.6 Compression bridge domain

Fig. 14.7 Optimal 2-D topology of compression bridge

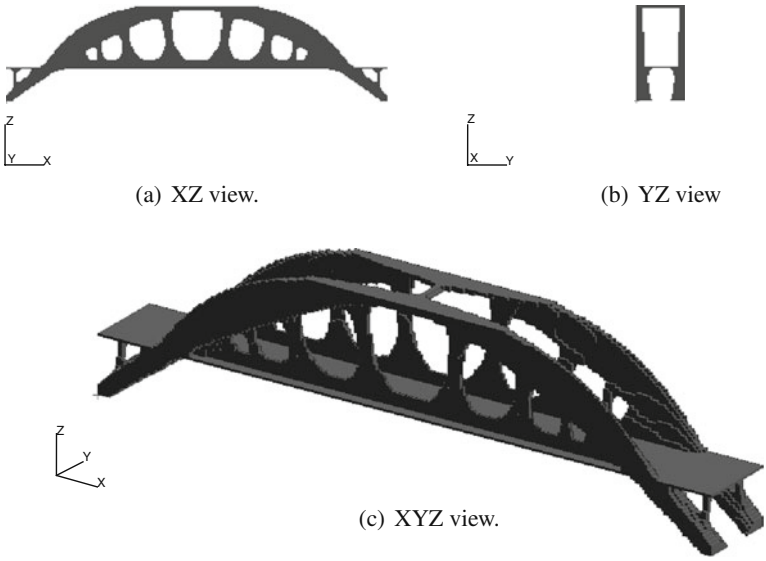

(a) XZ view. (b) YZ view

(c) XYZ view.

Fig. 14.8 Optimal 3-D topology of compression bridge

are supported each by a compression member, whereas the central span is suspended via a series of tension members. Different views for the three-dimensional version of the topology of the bridge are shown in Fig. 14.8. The topology obtained with the three-dimensional model presents some similarly, in the XZ plane, with the topology generated by the two-dimensional model (see Figs. 14.8(a) and 14.7) and with the design of the compression arch bridge reported in [28].

14.6.3 Example 3: Fiber Reinforce Cantilever Plate

To demonstrate the inclusion of the fibre-angle orientation in combined topology optimization environment, the in-plane design of cantilever plates with different material volume fractions is studied. The continuation method [29] is used in this

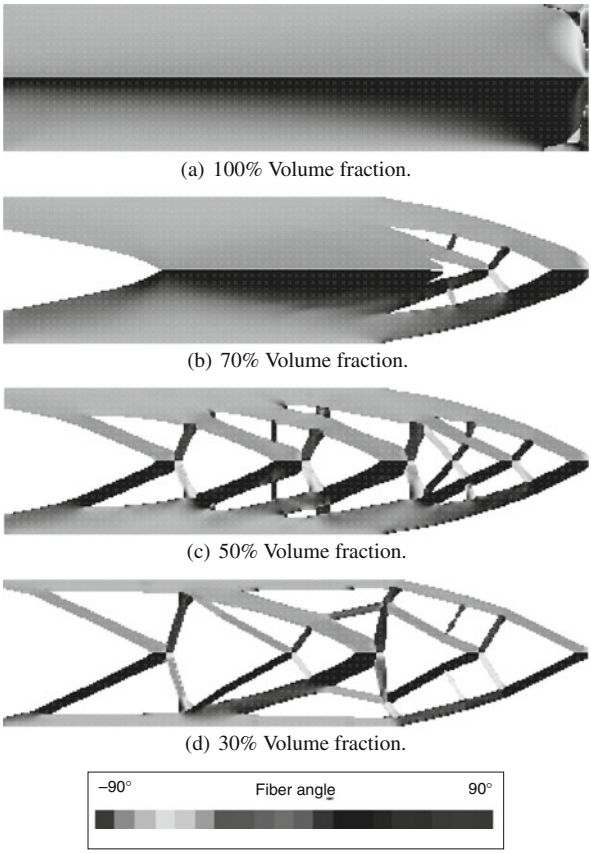

Fig. 14.9 Optimal topology of symmetric cantilever plate (325 × 82 cells) from [14]

study, with the penalization parameter p increasing gradually from 1.0 to 3.0 to avoid local minima. The following material are used:

$E_1 = 135.2$ GPa, $E_2 = 9.241$ GPa,
$G_{12} = 6.276$ GPa, $\nu_{12} = 0.318$.

The symmetric cantilever plate in Fig. 14.4 with an aspect ratio of 4 is modeled with a regular lattice of 325 × 82 cells. The topology optimization problem is solved using HCA scheme. Figures 14.9a through 14.9d show the topology of the optimal designs along with the color-coded fiber orientation angles for different volume fractions (for color version of this figure refer to [14]). These designs, as expected, are quite similar to classical optimal topologies of isotropic material (see example 1).

Corresponding to the designs shown in the figure, normalized compliances with respect to a 0° fiber design are tabulated in Table 14.2. These figures show that with the present choice of density interpolation scheme checkerboards are readily suppressed. Besides, for lower volume fractions, fibers are aligned with thin members similar to Mitchell type of structures.

Table 14.2 Normalized compliance of the symmetric cantilever for different volume fractions

Volume fraction	Normalized compliance
100%	0.74
70%	0.88
50%	1.14
30%	2.22

14.7 Concluding Remarks

Topology optimization of structures has matured enough to be often applied in industry, and continues to attract the attention of researchers and software companies in various engineering fields. Traditionally, most available algorithms for solving topology optimization problems are based on the global solution approach and require a large number of costly analyses. The CA paradigm offers a highly novel computational environment not only solving the topology design optimization problem efficiently, but also in terms of providing a flexible platform for design implementation of various practical constraints easily, which would otherwise render the traditional design approaches computationally infeasible. The main advantages of using the CA paradigm in structural design are the local analysis and design resolutions, and their massively parallel nature. The CA methodology can also take advantage of modern computational tools such as the multigrid acceleration method to improve their efficiency.

In this chapter, some applications of CA paradigm for structural design have been presented. The CA methodology was successfully applied to truss type and continuum structures. Some examples have been treated that illustrate the successes of the CA technique in solving topology optimization problems. Moreover, the multigrid accelerated CA scheme was shown to be an interesting candidate for solving topology optimization for continuum structures in a computationally efficient manner.

References

1. E. Kita, T. Toyoda, Structural design using cellular automata. Struct. Multidiscip. Optim. **19**, 64–73 (2000)
2. Y.M. Xie, G.P. Steven, A simple evolutionary procedure for structural optimization. Comput. Struct. **49**, 885–896 (1993)
3. C. Zhao, G.P. Steven, Y.M. Xie, Effect of initial non-design domain on optimal topologies of structures during natural frequency optimization. Comput. Struct. **62**, 119–131 (1997)
4. Z. Gürdal, B. Tatting, Cellular automata for design of truss structures with linear and non linear response. In *41st AIAA/ASME/ASCE/AHS/ASC Structures, Structural Dynamics and Materials Conference*, Atlanta, GA, 2000
5. R.T. Haftka, Z. Gürdal, *Elements of Structural Optimization*. (Kluwer, Dordrecht, 1993)
6. B. Tatting, Z. Gürdal, Cellular automata for design of two-dimensional continuum structures. In *8th AIAA/USAF/NASA/ISSMO Symposium on Multidisciplinary Analysis and Optimization*, Long Beach, CA, 2003
7. M.M. Abdalla, Z. Gürdal, Structural design using cellular automata for eigenvalue problems. Struct. Multidiscip. Optim. **26**, 200–208 (2004)

8. M.M. Abdalla, Z. Gürdal, Structural design using optimality based cellular automata. In *43th AIAA/ASME/ AHS/ASC Structures, Structural Dynamics and material Conference*, Denver, Co, April 2002
9. M. P. Bendsøe. Optimal shape design as a material distribution problem. Struct. Multidiscip. Optimi. **1**, 193–200 (1989)
10. M. Zhou, G.I.N. Rozvany, The COC algorithm, part II: Topological, geometry and generalized shape optimization. Comput. Meth. Appl. Mechan. Eng. **89**, 197–224 (1991)
11. G.I.N. Rozvany, M. Zhou, T. Birker, Generalized shape optimization without homogenization. Struct. Multidiscip. Optim. **4**, 250–252 (1992)
12. G.I.N. Rozvany, Aims, scope, methods, history and unified terminology of computer-aided topology optimization in structural mechanics. Struct. Multidiscip. Optim. **21**, 90–108 (2001)
13. O. Sigmund, A 99 line topology optimization code written in matlab. Struct. Multidiscip. Optim. **21**, 120–127 (2001)
14. S. Setoodeh, M.M. Abdalla, Z. Gürdal, Combined topology and fiber path design of composite layers using cellular automata. Struct. Multidiscip. Optim. **30**, 413–421 (2005)
15. R. Zakhama, M.M. Abdalla, H. Smaoui, Z. Gürdal, Topology design of geometrically nonlinear 2D elastic continua using CA and an equivalent truss model. In *11th AIAA/ISSMO Symposium on Multidisciplinary Analysis and Optimization*, Portsmouth, VA 2006
16. D.J. Slotta, B. Tatting, L.T. Watson, Z. Gürdal, S. Missoum, Convergence analysis for cellular automata applied to truss design. *Eng. Comput.* **19**, 953–969 (2002)
17. S. Setoodeh, D.B. Adams, Z. Gürdal, L.T. Watson, Pipeline implementation of cellular automata for structural design on message-passing multiprocessors. Math. Comput. Model. **43**, 966–975 (2006)
18. S. Kim, M.M. Abdalla, Z. Gürdal, M. Jones, Multigrid accelerated cellular automata for structural design optimization: A 1-D implementation. In *45th AIAA/ASME/ASCE/AHS/ASC Structures, Structural Dynamics and Materials Conference*, Palm Springs, CA, 2004
19. R. Zakhama, M.M. Abdalla, H. Smaoui, Z. Gürdal, Multigrid implementation of cellular automata for topology optimization of continuum structures. *CMES: Computer Modeling in Engineering and Sciences, to appear*, 2010
20. P. Wesseling, *An introduction to multigrid methods*. (Wiley, Chichester, 1992)
21. A. Tovar, N.M. Patel, G.L. Niebur, M. Sen, J.E. Renaud. Topology optimization using a hybrid cellular automaton method with local control rules. J. Mechan. Des. **128**(6), 1205–1216 (2006)
22. A. Tovar, N.M. Patel, A.K. Kaushik, J.E. Renaud, Optimality conditions of the hybrid cellular automata for structural optimization. AIAA J. **45**(3), 673–683 (2007)
23. S. Missoum, M.M. Abdalla, Z. Gürdal, Nonlinear topology design of trusses using cellular automata. In *44th AIAA/ASME/AHS/ASC Symposium on Structural Dynamics and Material Conference*, Norfolk, VA, 2003
24. S. Missoum, M.M. Abdalla, Z. Gürdal, Nonlinear design of trusses under multiple loads using cellular automata. In *5th World Congress in Structural and Multidisciplinary Optimization*, Lido diJesolo, Italy, 2003
25. S. Setoodeh, Z. Gürdal, L.T. Watson. Design of variable-stiffness composite layers using cellular automata. Comput. Meth. Appl. Mechan. Eng. **195**, 836–851 (2006)
26. N.V. Banichuk, Optimization of anisotropic properties of deformable media in plane problems of elasticity. *Mesh Solids*, **14**, 63–68 (1979)
27. P. Pedersen. Bounds on elastic energy in solids of orthotropic materials. Struct. Optim. **2**, 55–63 (1990)
28. M. Beckers, Topology optimization using a dual method with discrete variables. Struct. Optim. **17**, 14–24 (1999)
29. M.P. Bendsøe, O. Sigmund, *Topology Optimization, Theory, Methods and Applications* (Springer-Verlag, 2003)